ELSEVIER

Chemical Engineering Journal 86 (2002) 133–138

Chemical Engineering Journal

www.elsevier.com/locate/cej

On the risk of cracking in clay drying

F. Augier [a,*], W.J. Coumans [a], A. Hugget [a], E.F. Kaasschieter [b]

[a] *Laboratory of Separation Technology and Transport Phenomena, Eindhoven University of Technology, P.O. Box 513, 5600 MB Eindhoven, The Netherlands*

[b] *Department of Mathematics and Computing Science, Eindhoven University of Technology, P.O. Box 513, 5600 MB Eindhoven, The Netherlands*

Abstract

Based on the assumptions related to porous media, the governing equations of mass transfer and static equilibrium are presented. The mechanical stresses generated by the drying strains are expressed according to the linear-elastic model. The von Mises cracking criterion is introduced in order to locate the area where risk for cracking occurs. The model is applied to the drying of Kaolin clay. Moisture and solid displacements results as well as evolutions of the criterion are exposed. The danger of cracking is the highest at the beginning of the drying, since the yield stress is low. The criterion reaches its peak value during the first hour and at a particular point, located on the surface, exactly in-between two corners. Moisture evolution has been measured by means of nuclear magnetic resonance (NMR) imaging, during the drying of a piece of Kaolin clay. The diffusion coefficient is evaluated from these experimental results. Finally, the model is used to reproduce them. © 2002 Published by Elsevier Science B.V.

Keywords: Clay drying; Elasticity; Cracking criterion

1. Introduction

When the drying process takes place with shrinkage, gradients of moisture content and solid displacement in the material will lead to drying-induced stresses. Controlling these stresses is important since they can lead to undesired deformations and/or cracks affecting the product quality.

Mixture of clay and water is considered in a first assumption as perfectly elastic, because of the lack of data about the rheological properties of clay material. A model coupling mass transfer with stress balance, can permit to calculate the amount of stresses, according to several physical properties determined experimentally. The Huber–von Mises criterion is used to anticipate the crack appearance.

After the presentation of the mathematical model, a numerical formulation using the finite element method is developed and the results applied to clay brick drying are exposed and analysed. Cracking criterion evolutions allow to understand cracking occurrence. Finally, a validation of the diffusion model is given, by means of a comparison between the simulated and experimental data.

* Corresponding author. Tel.: +31-402-4736-74; fax: +31-402-4393-03.
E-mail address: f.f.augier@tue.nl (F. Augier).

2. The mathematical model

2.1. Assumptions

- Clay is a solid porous medium (density ρ_s) which can hold moisture (density ρ_m).
- Moisture may be present in clay indifferently as vapor, free or bound liquid.
- Temperature of clay form is uniform and constant.
- The effect of gravity is neglected.
- Clay material is isotropic.
- Mixture of clay and moisture shows a perfectly elastic behavior within the moisture range (0–0.4 g/g). This choice is a limiting assumption.

2.2. The diffusion model

As a shrinking medium, clay shows a movement of its solid skeleton while water moves through it. Using the moisture content M (kg water/kg dry solid) as state variable, moisture transport during clay drying is described by Eq. (1) where v_s (m/s) denotes the solid velocity, D (m^2/s) the diffusion coefficient of water in clay and J (kg/m^2 s) the moisture flux at the boundary surfaces exposed to drying conditions [1–4]:

$$\begin{aligned} &\frac{\partial M}{\partial t} + \boldsymbol{v}_s \nabla M = \frac{1}{\rho_s} \nabla \rho_s D \nabla M, && \text{in } \Omega \\ &J = -\rho_s D \nabla M \boldsymbol{n}, && \text{in } \Gamma \end{aligned} \tag{1}$$

1385-8947/02/$ – see front matter © 2002 Published by Elsevier Science B.V.
PII: S1385-8947(01)00279-0

Nomenclature

D	diffusion coefficient (m^2/s)
E	Young modulus (N/m^2)
$\boldsymbol{F}$	external stress (N/m^2)
J	prescribed drying flux (kg/m^2 s)
K	bulk modulus (N/m^2)
M	dry basis moisture content (kg/kg)
$\boldsymbol{n}$	surface normal vector
$\boldsymbol{v}$	velocity (m/s)
$\boldsymbol{w}$	displacement vector (m)
$\boldsymbol{x}$	spatial position (m)
z	solid-attached position (m)

Greek symbols

$\boldsymbol{\varepsilon}$	total strain tensor
$\boldsymbol{\varepsilon}^{\mathrm{e}}$	elastic strain tensor
$\boldsymbol{\varepsilon}^{M}$	strain tensor due to moisture removal
$\boldsymbol{\varepsilon}^{\sigma}$	mechanical strain tensor
λ, μ	Lamé coefficients (N/m^2)
ν	Poisson ratio
ρ	apparent bulk mass density (kg/m^3)
$\boldsymbol{\sigma}$	stress tensor (N/m^2)
ψ	shrinkage factor

where Ω is the space domain occupied by the medium and Γ its surface. In Eq. (1), coefficient D is defined in a solid-attached frame using the following Eq. (2) [3]:

$$\rho_{\mathrm{m}}\boldsymbol{v}_{\mathrm{m}} = \rho_{\mathrm{m}}\boldsymbol{v}_{\mathrm{s}} - \rho_{\mathrm{s}}D\nabla M \tag{2}$$

The Lagrangian description has been applied to (1) in order to have a fixed computational domain [2,3,5]. Transformation rules [6] permit to switch from space co-ordinate system $\boldsymbol{x}(t)$ to solid-attached co-ordinates $z = \boldsymbol{x}(0)$ and eliminate the solid movement term, by means of the deformation tensor $(\nabla_z \boldsymbol{x})^{\mathrm{C}}$. Deduced from the law of mass conservation, the following relation defines the shrinkage factor ψ as inverse of the volume ratio:

$$\det(\nabla_z \boldsymbol{x})^{\mathrm{C}} = \frac{\mathrm{d}V}{\mathrm{d}V_0} = \frac{\rho_{\mathrm{s}}^0}{\rho_{\mathrm{s}}} = \psi^{-1} \tag{3}$$

At this stage, an additional assumption is taken: deformation is only due to moisture removal, that is to say deformations due to mechanical stresses are smaller and therefore neglected. Hence, deformations are purely volumetric and $(\nabla_z \boldsymbol{x})^{\mathrm{C}}$ is a diagonal tensor. Furthermore, because of isotropy, $(\nabla_z \boldsymbol{x})^{\mathrm{C}}$ has equal diagonal elements:

$$(\nabla_z \boldsymbol{x})^{\mathrm{C}} = \psi^{-1/3}\boldsymbol{I} \tag{4}$$

After transformation and applying (4), Eq. (1) reads [1]:

$$\begin{aligned} &\left.\frac{\partial M}{\partial t}\right|_z + \nabla_z(D\nabla_z M), \quad \text{in } \Omega \\ &-\rho_{\mathrm{s}}^0 D\nabla_z M\boldsymbol{n} = J, \qquad \text{in } \Gamma \end{aligned} \tag{5}$$

where $D = \psi^{2/3}D$ and $J = \psi^{-2/3}J$. Adding the initial condition, $M(z, t = 0) = M^0$, $z \in \Omega$, Eq. (5) correspond to the mathematical formulation of the diffusion problem.

2.3. The stress model

Let $\boldsymbol{\varepsilon} = \nabla\boldsymbol{w} + \nabla\boldsymbol{w}^{\mathrm{C}}$ be the total strain tensor, function of the solid displacements $\boldsymbol{w} = \boldsymbol{x}(t) - z$. With the assumption of a constant and uniform temperature, the total strain is reduced to the sum of the elastic strain and the shrinkage due to moisture [7], given as follows:

$$\boldsymbol{\varepsilon} = \boldsymbol{\varepsilon}^{\sigma} + \boldsymbol{\varepsilon}^{M} \tag{6}$$

The assumption of local isotropic shrinkage reads $\boldsymbol{\varepsilon}^{M} = \boldsymbol{\varepsilon}^{M}\boldsymbol{I}$.

For an isotropic material, Hook's law describes the elastic strain as follows:

$$\boldsymbol{\varepsilon}^{\sigma} = \boldsymbol{\varepsilon}^{\mathrm{e}} = \frac{1+\nu}{E}\boldsymbol{\sigma} - \frac{\nu}{E}\mathrm{Tr}(\boldsymbol{\sigma})\boldsymbol{I} \tag{7}$$

where E and ν are the moisture-dependent elastic properties of the mixture.

The balance of momentum for a static equilibrium reads:

$$\nabla\boldsymbol{\sigma} + \boldsymbol{F} = 0$$

By assumption, no external forces are applied to the clay body.

$$\nabla\boldsymbol{\sigma} = 0 \tag{8}$$

On Γ, the boundary condition reads:

$$\boldsymbol{\sigma}n = 0$$

Inverting (7) and introducing (6), the momentum balance (8) and the boundary condition can be written in term of strains:

$$\begin{aligned} &\nabla(\lambda\,\mathrm{Tr}(\boldsymbol{\varepsilon})\boldsymbol{I} + 2\mu\boldsymbol{\varepsilon} - 3K\boldsymbol{\varepsilon}^{M}\boldsymbol{I}) = 0, \quad \text{in } \Omega \\ &(\lambda\,\mathrm{Tr}(\boldsymbol{\varepsilon})\boldsymbol{I} + 2\mu\boldsymbol{\varepsilon} - 3K\boldsymbol{\varepsilon}^{M}\boldsymbol{I})\boldsymbol{n} = 0, \quad \text{in } \Gamma \end{aligned} \tag{9}$$

where λ, μ, and K are properties of the mixture, functions of E and ν (Eq. (9)) correspond to the mathematical formulation of the stress problem and its solution consists of the displacement $\boldsymbol{w}$ at the instant t. To solve this set of Eq. (9), the moisture content need to be known everywhere, so the diffusion problem should be solved at first.

3. Simulation

Based on the previous model, simulations of clay brick drying have been ran using the finite element method, in order to study the crack occurrence.

3.1. Problem configuration

We apply the mathematical model to a Kaolin clay brick submitted to drying with an initial moisture content of

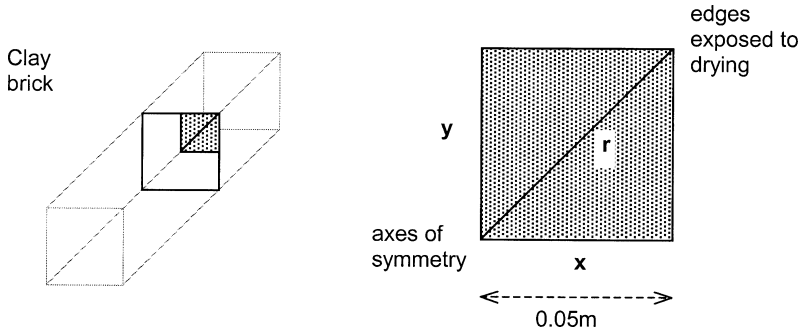

Fig. 1. Spatial configuration.

0.4 g/g. Eqs. (5) and (9) are solved on a two-dimensional mesh representing the quarter (0.05 cm × 0.05 cm) of a cross-section of the clay brick, as shown on Fig. 1. Hence, the brick is assumed to have an infinite length. The mesh consists of 80 × 80 rectangular elements.

3.2. Physical properties

Moisture-dependent physical properties needed by the model were obtained experimentally [3,8].

The shrinkage factor $\psi(M)$ defined in Eq. (3), decreases linearly from $M = 0.4$ g/g to a critical moisture content $M_c = 0.27$ g/g and then remains constant. Indeed, clay drying consists in two phases: the shrinkage for $M > M_c$ where solid particles slip into a more compact arrangement [9], and the non-shrinking phase for $M < M_c$ where solid density stays nearly constant.

The diffusion coefficient D for Kaolin clay has been determined experimentally from one-dimensional drying experiments. Experimental data and the approximation of D using artificial neuronal network [1] are given Fig. 2. The prescribed drying flux J is derived from drying curves.

Compression tests at different moisture contents have led to an approximation of the Young's modulus E (Fig. 3). Poisson's coefficient is taken equal to 0.45.

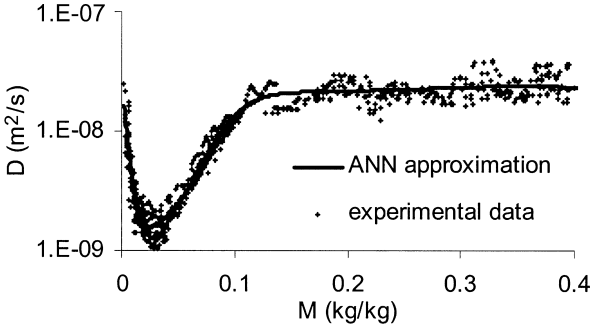

Fig. 2. Diffusion coefficient for Kaolin clay at 25 °C, obtained from one-dimensional NMR profiles.

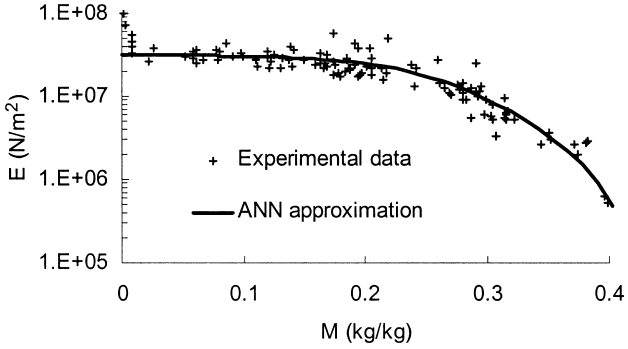

Fig. 3. Young's modulus for Kaolin clay [3].

4. Results and discussions

Numerical results consist firstly of the moisture content evolution inside the two-dimensional section, and secondly of displacements of the material points at different time-steps. From the displacements, total and elastic strains and thus stresses are derived, which permits to calculate a cracking criterion. On Figs. 4–10, the legend refers to the drying hours.

4.1. Moisture and displacements

Fig. 4 shows moisture evolution along the diagonal of the slice. During the first drying stage moisture content

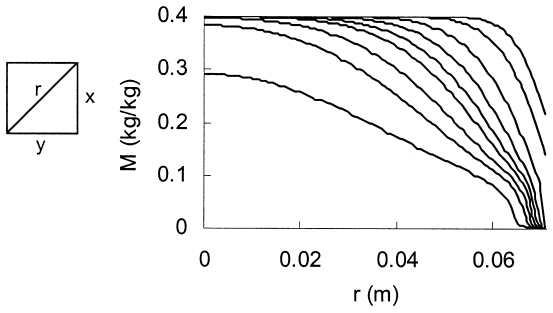

Fig. 4. Moisture evolution along r-direction (at different drying hours).

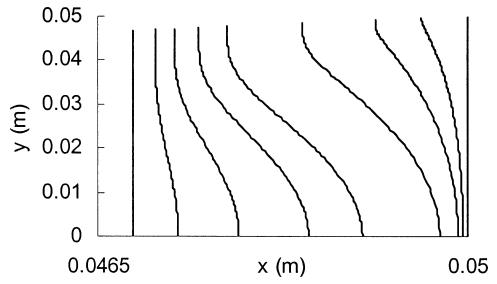

Fig. 5. Displacements of the edge $x(t = 0) = 0.05$ (at different drying hours).

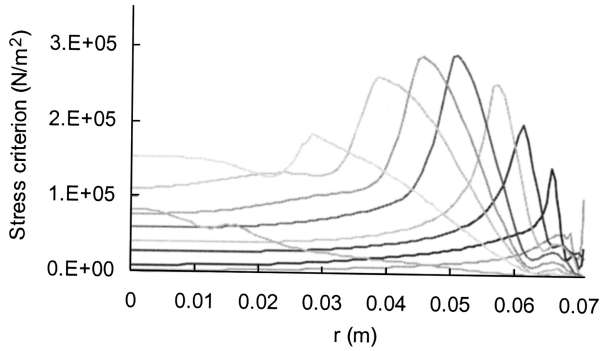

Fig. 6. Stress criterion along the r-direction (at different drying hours).

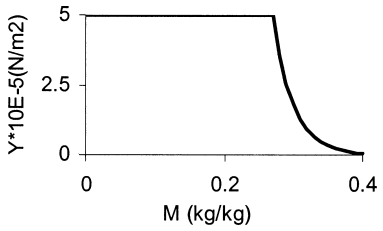

Fig. 7. Yield stress for Kaolin clay.

decreases fast, especially in the corner where evaporation surface is important. We notice a slope break around 0.1 kg/kg, due to the evolution of D (Fig. 2). After about 1 h of drying, a penetrating drying front appears inside the material, consequence of the increase of D at very low moisture contents (predominant vapor flow inside the pores).

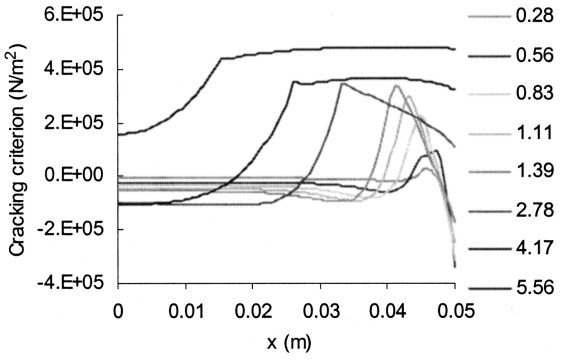

Fig. 8. Cracking criterion along the x-direction (drying times in hours).

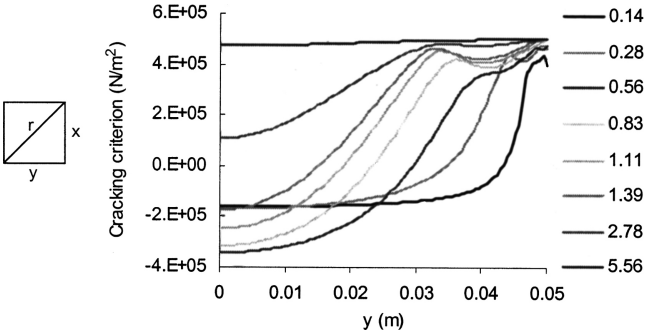

Fig. 9. Cracking criterion along the y-direction (drying times in hours).

Fig. 5 shows the displacement of the edge exposed to drying air. Because of its high drying rate, the corner undergoes a large strain at the beginning. It induces a deformation gradient from $y = 0$–0.05 and until 5 h of drying. After this time, solid movement stops and the material returned to its initial shape. Indeed, below $M_c = 0.27$ g/g, volumetric strain ceases and, as a consequence of the linear elastic assumption, stress and elastic strain disappear: all solid particles have undergone the same strain.

4.2. Stress analysis

The conditions that lead to cracking can be determined by using a specific criterion. Since the crack appearance is independent of the hydrostatic pressure, we consider only the deviatoric part of the stress tensor, written down $\bar{\sigma}$. Then, because of isotropic behaviour, the second invariant of $\bar{\sigma}$ is used. Hence, we will first focus on the following expression, called here the "stress criterion" and corresponding to the second invariant of the deviatoric part of the stress tensor:

$$\sqrt{\tfrac{3}{2}\mathrm{Tr}(\bar{\sigma}^2)}$$

Fig. 6 shows the evolution of the stress criterion along the diagonal r of the section. Each profile shows a peak corresponding to the location where $M = M_c$, that is to say where strains have reached a maximum value (end of the shrinking phase). For each profile, above and below $M = M_c$, the stress criterion is lower: above M_c (inner part), displacements and strains have not yet reached the maximum. Below M_c (outer part) total strain becomes uniform which induces a decrease of stress.

The Huber–von Mises yield criterion is proposed for problems in which frictions are not important [10]. This criterion states that in order to prevent cracking the following condition have to be satisfied:

$$Y - \sqrt{\tfrac{3}{2}\mathrm{Tr}(\bar{\sigma}^2)} > 0 \tag{10}$$

where $Y(M)$ is the moisture-dependant yield stress, limit of the elastic behaviour of the material when submitted to a uniaxial tension. For Kaolin, Y has been determined experimentally by Ketelaars (Fig. 7).

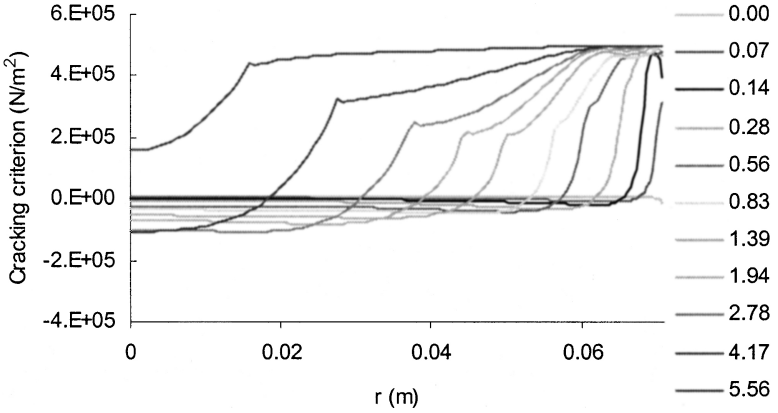

Fig. 10. Cracking criterion along the *r*-direction (drying times in hours).

Figs. 8–10 show the evolution of the cracking criterion along the *x*-, *y*- and *r*-directions. Danger for cracking appears when the criterion is negative and increases with its absolute value. We notice from Figs. 8 and 9 that maximum danger occurs at $x = 0.05$ and $y = 0$, at time 0.56 h. The risk remains important in this location during approximately the first 1.5 h of drying. Danger is located especially on the edge (Fig. 8; $x = 0.05$) around the axis of symmetry ($y = 0$) of the brick (Fig. 9). As shown in Fig. 10, the criterion is higher inside the slice. After 1.5 h of drying, risk for cracking is low everywhere.

The location of danger results from the drying rate difference between the corner and the middle of the edge, which induces important strain gradients along the edge (Fig. 5). Thus, the area around $x = 0.05$ and $y = 0$ undergoes large tensile stress. Besides, at the beginning of the drying the yield stress is low because of the high moisture content. Combining this large tensile stress with the low yield stress, the danger for cracking becomes important.

5. Experimental approach

The model and crack anticipation need to be validated by means of experiments. We present a result corresponding to the diffusion problem.

5.1. 2-Dimensional moisture measurements using NMR imaging

A drying experiment using nuclear magnetic resonance (NMR) has been carried out on a Kaolin clay sample. With the objective to reproduce the corner of a brick, precautions are taken to ensure that moisture movement occurs in two dimensions. The sample has a right-angled triangle shape, as it can be noticed in Fig. 11, and both upper edges are identically exposed to a longitudinal drying airflow. The experimental data consist of the evolution with time of a two-dimensional moisture field.

Fig. 11 shows the evolution of moisture qualitatively; light color corresponding to high moisture contents and dark to the absence of moisture. Both right and left sides of the sample have the same symmetric behavior. It appears clearly that the moisture in the corner decreases faster than along the edge. Since moisture content is above 0.27 g/g, it induces strain gradients between the corner and the middle of the edge, involving stresses. Differential strains on boundaries can be noticed on the first pictures.

5.2. Diffusion coefficient from a two-dimensional moisture evolution

The diffusion coefficient defined in system (1) has been calculated from the results of the two-dimensional experiment (Fig. 11), using a method based on the assumption that *D* depends only on the moisture content. Flux and gradients are obtained along iso-moisture lines in order to calculate *D*. Results are showed in Fig. 12. The range of moisture content is reduced for two reasons. First, the shrinkage is not taken into account for the calculations and second profiles measured at the beginning of the drying are too flat to get accurate gradients.

The coefficient used for the simulation (Fig. 2) is very near to this result in the moisture range (0–0.12 g/g).

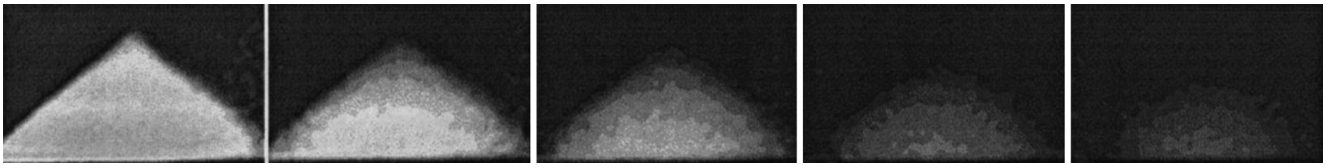

Fig. 11. NMR imaging of clay drying (time: 0–1.5–3–5–10 h; drying air specifications: 0% RH, 1.7 m/s, room temperature (19 °C).

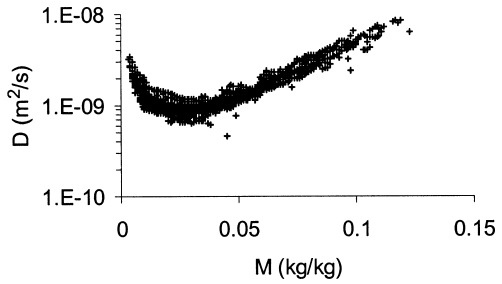

Fig. 12. Diffusion coefficient from two-dimensional moisture profile evolution.

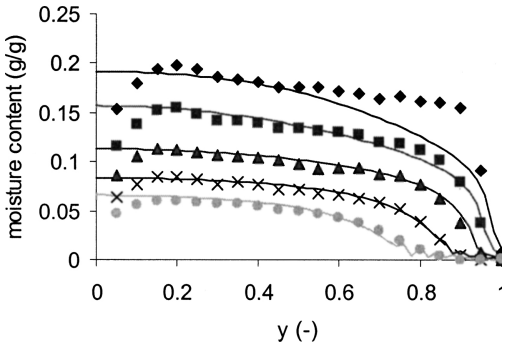

Fig. 13. Comparison between theory (lines) and experience (points). Profile times: 42, 98, 182, 322, 504 min.

We notice that D from the two-dimensional drying is lower, what is explained by the difference of temperature between both experiments (about 5 °C). The agreement permits to validate the assumption of isotropy. Besides, results from the two-dimensional test are more accurate, because the method induces less averages than the one-dimensional experiment, by taking into account the boundary effects.

5.3. Comparison between the model and experiment

The parameters have been tuned to study how far the model can reproduce the experiment, and be validated by this way. Boundary drying fluxes have been found by integrating moisture profiles along the axis of symmetry of the sample, where it is assumed that no perpendicular gradients take place. Fig. 13 shows the evolution of moisture content along the y-axis of the slice, plotted in a fixed unit. The experiment is well reproduced by the model, all along the drying stage. Low experimental points near the origin ($y = 0$) correspond to inaccuracies of the NMR signal, far from the center of the magnets. These errors cannot be seen clearly on Fig. 11, because of some data averaging.

6. Conclusions

From a mathematical model including moisture transport in porous medium and balance of momentum for static equilibrium, a numerical solution is obtained by means of the finite element method. Both, the moisture content evolution and solid displacements are calculated all over a cross-section of a Kaolin clay brick. Since the material is assumed to be perfectly elastic, strains and stresses are obtained and the Huber–von Mises cracking criterion is analyzed. Maximum risk for cracking occurs at the surface around the axe of symmetry of the brick and, according to the drying conditions applied, after 0.56 h of drying.

A validation of the diffusion model is given, based on the calculation of the diffusion coefficient from a two-dimensional moisture evolution measured by NMR. A good agreement has been found between the coefficient from the one-dimensional drying tests and from the two-dimensional NMR experiment, for the non-shrinking phase. We aim to generalize these two-dimensional calculations for the whole drying process and to increase the accuracy of the method, which could be applied favorably to products with a more complex shape.

The experimental study of crack appearance is now in progress, in order to estimate the stress model and the use of the cracking criterion. For the improvement of the stress model, more rheological properties, such as viscosity, need to be known all over the moisture range. This supposes to realise the mechanical tests before simulating the viscous behavior.

References

[1] A. Hugget, W.J. Coumans, E.F. Kaasschieter, Reports on applied and numerical analysis RANA 99–30, Eindhoven University of Technology, 1999.
[2] A. Wigmans, A model for Drying Process of Clay, Master's Thesis, Eindhoven University of Technology, 1994.
[3] A.A.J. Ketelaars, Drying deformable media: kinetics, shrinkage and stresses, Ph.D. Dissertation, Eindhoven University of Technology, 1992.
[4] W.J. Coumans, Power law diffusion in drying processes, Ph.D. Dissertation, Eindhoven University of Technology, 1987.
[5] E.F. Kaasschieter, Een eindige elementmethode voor het modelleren van het drogen van kleivormlingen, Eindhoven University of Technology, 1992.
[6] P. Chadwick, Continuum Mechanics, George Allen & Unwin, London, 1976.
[7] S.J. Kowalski, Int. J. Eng. Sci. 34 (13) (1996) 1491–1506.
[8] B. Kroes, The Influence of Material Properties on Drying Kinetics, Ph.D. Dissertation, Eindhoven University of Technology, 1999.
[9] G. Onoda, E.G. Liniger, M.A. Janney, Ceram. Trans. 1: Ceram. Powder Sci. II (1988) 611–623.
[10] J. Irudayaraj, K. Haghighi, R. Stroshine, Dry. Technol. 11 (5) (1993) 901–959.